

A first-principles investigation into the ferroelectric and antiferrodistortive instabilities of cubic SrTiO₃

This article has been downloaded from IOPscience. Please scroll down to see the full text article.

2007 J. Phys.: Condens. Matter 19 506213

(<http://iopscience.iop.org/0953-8984/19/50/506213>)

View [the table of contents for this issue](#), or go to the [journal homepage](#) for more

Download details:

IP Address: 129.252.86.83

The article was downloaded on 29/05/2010 at 06:58

Please note that [terms and conditions apply](#).

A first-principles investigation into the ferroelectric and antiferrodistortive instabilities of cubic SrTiO₃

Ying Xie¹, Hong-gang Fu^{1,4}, Hai-tao Yu², Guo-xu Zhang² and Jia-zhong Sun^{2,3}

¹ Department of Applied Chemistry, Harbin Institute of Technology, Harbin 150001, People's Republic of China

² School of Chemistry and Materials Science, Heilongjiang University, Harbin 150080, People's Republic of China

³ State Key Laboratory of Theoretical and Computational Chemistry, Institute of Theoretical Chemistry, Jilin University, Changchun 130023, People's Republic of China

E-mail: fuhg@vip.sina.com

Received 29 August 2007, in final form 24 October 2007

Published 20 November 2007

Online at stacks.iop.org/JPhysCM/19/506213

Abstract

The lattice dynamics and potential energy curves of cubic SrTiO₃ as a function of lattice volume were investigated by density functional theory (DFT) calculations. The calculated results indicate that the lowest optical phonon in the Brillouin-zone center is real and an unstable R₂₅ mode, corresponding to the antiferrodistortive transition, is found at the equilibrium volume. The results are consistent with previous experimental predictions. Moreover, increasing volume can improve the ferroelectric instability and restrain the antiferrodistortive one. A competition between the ferroelectric and antiferrodistortive instabilities does exist. The smaller lattice constant of cubic SrTiO₃ than of BaTiO₃ is crucial both for the appearance of the antiferrodistortive instability and the disappearance of the ferroelectric instability, which makes the transition behaviors of the two compounds entirely different.

(Some figures in this article are in colour only in the electronic version)

1. Introduction

During the past several decades, SrTiO₃ has been an attractive subject of many experimental and theoretical investigations [1–7]. It behaves as an incipient ferroelectric and first undergoes an antiferrodistortive (AFD) transition when the temperature drops below 110 K [1]. As the temperature continuously decreases, its dielectric constant increases sharply. This increase appears to obey the Curie–Weiss law, being consistent with an impending ferroelectric (FE)

⁴ Author to whom any correspondence should be addressed.

transition at about 20 K [2]. However, SrTiO₃ does not become FE phase but still remains tetragonal structure ($I_{4/mcm}$) as the temperature approaches 0 K [2–4].

This particular behavior that the system fails to condense into an FE phase has attracted much theoretical attention [5–8]. Lasota and co-workers have calculated the phonon band of cubic SrTiO₃ [5]. Although they correctly predicted the well-known instability at the R point of the Brillouin zone, the calculation at the Γ point was not satisfactory because the results clearly indicated that the FE Γ_{15} mode with an imaginary frequency of -100 cm^{-1} is more unstable than the AFD R_{25} mode [5]. Relying on the local density approximation (LDA) technique, Zhong and co-workers investigated the role of Coulomb interactions in eight ABO₃ perovskite compounds, and they also found an unstable Γ_{15} mode with an imaginary frequency of -41 cm^{-1} in the cubic lattice of SrTiO₃ [6]. However, for SrTiO₃, no FE phase can be observed experimentally [2–4]. Further theoretical investigations confirmed that the FE transition at low temperature is completely suppressed because of the so-called quantum paraelectric behavior [7, 8]. Since previous LDA calculations did not give a satisfactory result with experiments, we present here a GGA calculation on the phonon frequencies at highly symmetrical k -points of the Brillouin zone. Moreover, Cohen investigated the ferroelectricity of perovskite oxides and pointed out that the hybridization between Ti_{3d} and O_{2p} states is essential for the ferroelectricity of BaTiO₃ and PbTiO₃ [9]. However, the existence of a Ti–O covalent bond in SrTiO₃ [10] does not lead to a similar behavior, and the origin of the AFD instability in SrTiO₃ still remains unclear. Therefore, further investigation is very necessary. Considering that the substitution of Ba by Sr leads to a significant change in lattice constant [11], it is reasonable to investigate the vibrational properties of SrTiO₃ as a function of the lattice constant.

With these motivations, the present investigation is aimed at providing an application of first-principles techniques to obtain the volume dependence of the vibrational properties and distinguish the phase transition behavior of SrTiO₃ from BaTiO₃.

2. Theory and computation details

The present calculations were performed in the density functional theory (DFT) framework [12] implemented in the CASTEP package [13]. The exchange–correlation energy was treated with the Perdew–Wang functional [14] in the generalized gradient approximation (GGA) scheme. The electronic wavefunctions were expanded in terms of a plane-wave (PW) basis set, and the used energy cutoff is 660 eV. With the application of norm-conserving pseudopotentials, the original valence configurations are $3d^2 4s^2$ for Ti, $4s^2 4p^6 5s^2$ for Sr, and $2s^2 2p^4$ for O. The sampling over the Brillouin zone was treated by a $(6 \times 6 \times 6)$ Monkhorst–Pack mesh [15].

As depicted in figure 1, two models, a simple cubic structure and a pseudo $I_{4/mcm}$ structure, were considered in the present study. The pseudo $I_{4/mcm}$ structure refers to that possessing a tetragonal lattice constant but no rotational displacements. The equilibrium configuration is firstly located by geometry optimization, and then, the phonon frequencies at different highly symmetrical k points of the Brillouin zone are obtained from the linear-response calculations [16]. The phonons at different volumes and the AFD distortion dependence of the total energy are computed and analyzed.

Furthermore, for investigating how volume change affects the long-range dipolar contribution to the lattice dynamics [16, 17], the dynamical charge tensor, defined as the coefficient between the macroscopic polarization (P_β) in direction β and a rigid displacement (τ) of atom k in direction α multiplied by the unit cell volume (V_0) [16, 17],

$$Z_{k,\alpha\beta}^* = V_0 \frac{\partial P_\beta}{\partial \tau_{k,\alpha}} \quad (1)$$

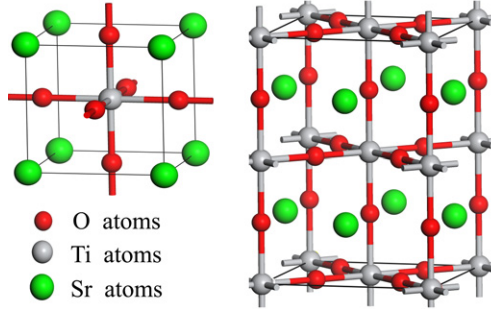


Figure 1. Calculation models for SrTiO₃.

Table 1. Computed and experimental lattice parameter (a_0 , Å), bulk modulus (B_0 , GPa) for cubic SrTiO₃.

	Present ^a	LAPW ^b	Expt. ^c
a_0	3.922	3.922	3.903
B_0	192	190	183

^a The equilibrium volume is 60.33 Å³.

^b Reference [5]: linear-augmented plane-wave calculations.

^c a_0 and B_0 are taken from [18] and [19], respectively.

is considered. In a crystal with periodic boundary conditions, because the change of polarization also depends on the boundary condition fixing the macroscopic electric fields (ε), equation (1) can be rewritten as,

$$Z_{k,\alpha\beta}^* = V_0 \left. \frac{\partial P_\beta}{\partial \tau_{k,\alpha}} \right|_{\varepsilon=0} + V_0 \sum_j \frac{\partial P_\beta}{\partial \varepsilon_j} \frac{\partial \varepsilon_j}{\partial \tau_{k,\alpha}}. \quad (2)$$

As the electrostatics imposes a relationship between macroscopic polarization, and electric and displacement fields [16, 17],

$$D_\alpha = \varepsilon_\alpha + 4\pi P_\alpha = \sum_j e_{\alpha,j}^\infty \varepsilon_j \quad (3)$$

the dynamical charge is determined by

$$Z_{k,\alpha\beta}^* = V_0 \left. \frac{\partial P_\beta}{\partial \tau_{k,\alpha}} \right|_{\varepsilon=0} + V_0 \sum_j \frac{(e_{\beta,j}^\infty - \delta_{\beta,j})}{4\pi} \frac{\partial \varepsilon_j}{\partial \tau_{k,\alpha}} \quad (4)$$

where $e_{\beta,j}^\infty$ represents the electronic contribution to the dielectric tensor. Therefore, the Born effective charge (BEC) referring to the polarization change caused by atomic displacements at zero macroscopic electric fields [16, 17] can be calculated by

$$Z_{k,\alpha\beta}^* = V_0 \left. \frac{\partial P_\beta}{\partial \tau_{k,\alpha}} \right|_{\varepsilon=0}. \quad (5)$$

3. Results and discussion

The optimized lattice parameter and bulk modulus of cubic SrTiO₃, together with other theoretical [5] and experimental values [18, 19], are listed in table 1. The optimized equilibrium lattice constant (3.922 Å) showed in figure 2 is only 0.5% larger than the experimental

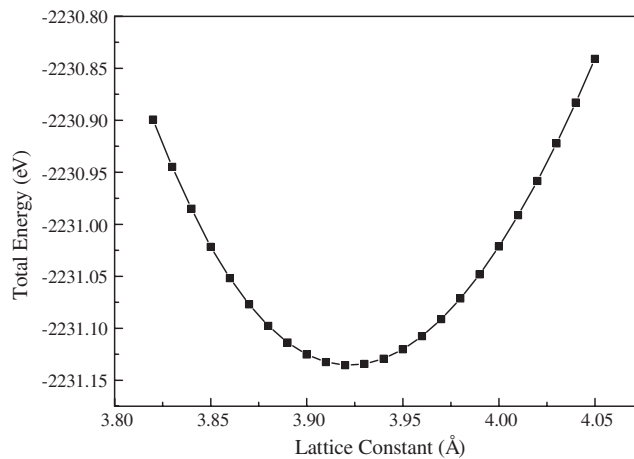


Figure 2. Total energy of cubic SrTiO₃ as a function of lattice constant.

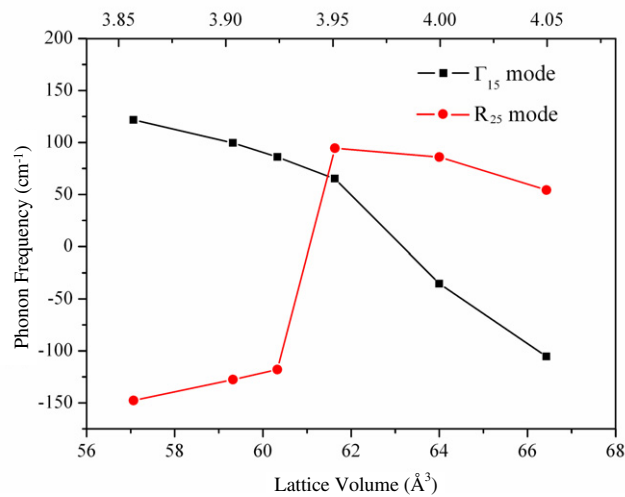


Figure 3. Volume dependence of phonon frequencies at the Γ and R points of the Brillouin zone.

value (3.903 Å) [18] and is consistent with previous theoretical predictions [5]. However, the computed optical dielectric constant of 6.11 is overestimated by comparison with the experimental value of 5.83 [20]. The origin of this error is very complex and it arises at least partly from the lack of polarization dependence of the approximate exchange–correlation functional [21]. By improving the functional, the optical dielectric constant is improved, as can be noted from the fact that the present GGA value (6.11) is closer to the experimental value (5.83) than the previous LDA result (6.63) [5]. Moreover, because the inaccuracy of the optical dielectric constant only significantly affects the position of the highest longitudinal optical branch [5, 22], the discussions on the low frequency phonons below are not affected.

Figure 3 shows the volume dependence of phonon frequencies at Γ and R points of the Brillouin zone. The unstable modes, which determine the nature of phase transitions, are characterized by negative values. At equilibrium volume (60.33 Å³), the lowest optical phonon

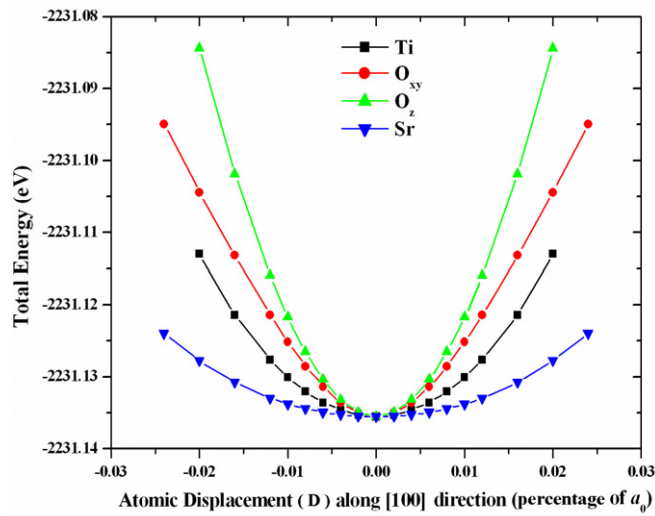


Figure 4. Total energy versus FE distortion amplitude (atomic displacements, D) at equilibrium volume (60.33 \AA^3).

(Γ_{15} mode) at the Brillouin-zone center remains real (86 cm^{-1}), indicating the absence of FE instability in cubic SrTiO_3 . This result differs from early theoretical calculations, in which the unstable FE A_{1u} mode was predicted to be -41 and -100 cm^{-1} [5, 6]. According to experiments, the static dielectric response of SrTiO_3 above 50 K appears to obey the Curie–Weiss law, suggesting an impending FE transition at low temperatures [2]. However, SrTiO_3 does not turn into the FE phase but still remains a tetragonal ($I_{4/mcm}$) structure when the temperature approaches 0 K [2–4]. The experimental results above suggested that the FE instability should be rather weak even if it exists. Moreover, further theoretical investigations confirmed that the FE transition at low temperature is completely suppressed because of the quantum paraelectric behavior [7, 8]. Therefore, the disagreement between the LDA [5, 6] and experimental results [2, 4] may result from the bad estimation for the exchange–correlation energy. Figure 4 depicts the total energy change with respect to atomic displacements. The result clearly indicates that the displacements of Sr, Ti, and O atoms along the FE mode eigenvector uniquely produce a single well, being consistent with the absence of FE instability. The total energy calculation results are in good agreement with the potential energy surfaces of Ti and Sr displacements in cubic SrTiO_3 [11].

The computed phonons at highly symmetrical k points of the Brillouin-zone boundary are listed in table 2, and the symmetry labels follow the convention of [23]. The result shows that the most unstable phonon located at the R point equals -118 cm^{-1} . This phonon denoted as the R_{25} mode is found to be triply degenerate, and the associated eigenvector only contains the displacements of O atoms. In reciprocal space, it is found that the eigenvector of the R_{25} mode is along the diagonal of the cubic face as visualized in the inset of figure 5. Owing to the symmetry constraint, the three O atoms in the cubic phase are equivalent, therefore the eigenvector of the R_{25} mode is confined to a quasi-one-dimensional ‘tube’ (circles in the second inset of figure 5). In real space, this instability is characterized by opposite rotations of oxygen octahedrons in adjacent cells. Figure 5 shows the computed values of total energies versus rotational displacements of the R_{25} mode. At equilibrium volume (60.33 \AA^3), the total energy curve clearly shows a typical double-well characteristic, being consistent with the result by Sai

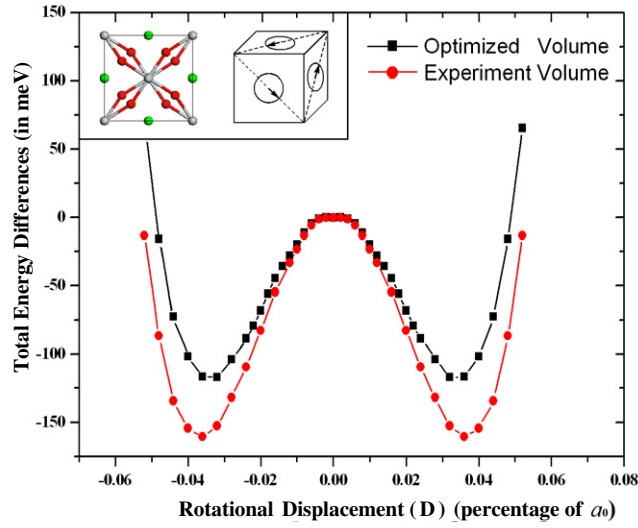


Figure 5. Total energy as a function of rotational displacement (D) of the R_{25} mode at different volumes. The inset shows a sketch of the AFD distortion in real and reciprocal spaces.

Table 2. Phonon frequencies at highly symmetrical k -points of the Brillouin-zone boundary at equilibrium volume (60.33 \AA^3). Symmetry labels follow the convention of [23].

Phonon	M point	X point		R point	
	Frequencies (cm^{-1})	Phonon	Frequencies (cm^{-1})	Phonon	Frequencies (cm^{-1})
M_3	−93	X_5	86, 205, 551	R_{25}	−118
M'_2	87	X'_5	138, 276	R_{15}	113, 391
M'_5	94, 247, 475	X_2	155	R'_{25}	447
M'_3	174, 531	X_1	243	R'_{12}	551
M_5	282	X_3	275	R'_2	859
M'_1	419	X'_2	784		
M_2	570				
M_4	828				

and Vanderbilt [24]. According to the soft-mode theory, when the temperature drops below the Curie temperature, the O atoms are trapped at the energy minimum and the corresponding phonon is condensed, leading to the occurrence of the AFD phase transition. Moreover, as the opposite rotations of oxygen octahedra do not bring any ferroelectricity, this AFD transition is of non-polar characteristic and therefore has little influence on the dielectric properties. Except for the unstable R_{25} mode, the M point also produces an unstable phonon. But this unstable phonon (M_3) was temperature-independent through the AFD transition [5].

To obtain an insight into the different phase transition behaviors between SrTiO_3 and BaTiO_3 , it is necessary to examine the effect of structural differences on the vibrational properties. Figure 3 clearly shows that the Γ_{15} mode becomes soft while the R_{25} mode turns hard with increasing volume. At expanded volume (experimental volume of BaTiO_3 , 64.48 \AA^3),

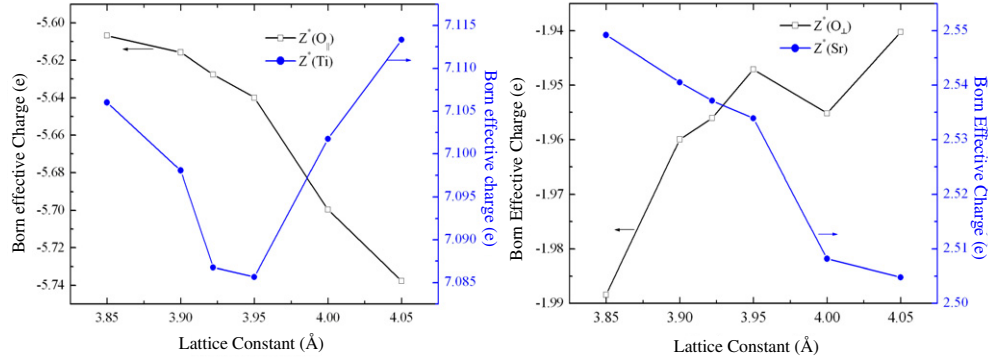


Figure 6. Born effective charge of each atom as a function of lattice constant.

an unstable FE phonon (-45 cm^{-1}) appears in the cubic lattice of SrTiO₃. Along with the appearance of this FE mode, however, the lowest phonon frequency at the R point is calculated to be 78 cm^{-1} , suggesting the disappearance of the corresponding AFD instability. Moreover, figure 5 also shows that the well depth increases from 117.1 to 160.6 meV with decreasing volume, confirming the enhancement of the AFD instability at compressing volume. Owing to the opposite volume dependence of the Γ_{15} and R_{25} modes, the competition between the FE and AFD instability does exist in cubic SrTiO₃. The results above are consistent with the conclusion that increasing pressure tends to enhance the AFD instability while suppressing the FE instability of perovskites, as expected from previous Monte Carlo simulations by Zhong and Vanderbilt [25].

Figure 6 shows the BEC of each atom as a function of lattice volume. For Sr and Ti atoms, their BECs are isotropic, owing to the symmetry. For oxygen, two independent values labeled as $O_{||}$ and O_{\perp} , which refer to the polarization change induced by displacements of O atoms parallel and perpendicular to the Ti–O bond respectively, must be considered. Our computation results indicate that $Z^*(\text{Ti})$ and $Z^*(O_{||})$ (figure 6(a)) deviate significantly from their nominal values expected from the purely ionic picture. Relying on the band-by-band decomposition technique, Ghosez and co-workers have investigated the BECs of seven ABO₃ perovskites, and their results suggested that such large anomalous values originating from the off-site orbital hybridization change are very common for this class of compounds [17]. Moreover, our results also show that $Z^*(\text{Sr})$ and the associated $Z^*(O_{\perp})$ (figure 6(b)) are close to their ionic charges, implying that the covalence of the Sr–O bond is rather weak. The calculated BECs are consistent with other theoretical predictions [5, 6, 17].

Figure 6(a) also shows that the absolute value of $Z^*(O_{||})$ monotonically increases with increasing volume and $Z^*(\text{Ti})$ also increases when the lattice constant is larger than 3.950 Å. This variation trend indicates that the long-range interactions between Ti and O atoms are enhanced, while the short-range repulsions between them are weakened as the lattice volume increases. In ABO₃ compounds, it is believed that the phase transition is controlled by a delicate balance between a long-range Coulomb force, which favors the low-symmetry configurations, and short-range repulsion, which reserves the high-symmetry structures [9]. Therefore, the changes in $Z^*(O_{||})$ and corresponding $Z^*(\text{Ti})$ with increasing volume actually reflect the interaction change of the Ti–O pair, which can be responsible for the appearance of the FE mode at expanded volume. On the contrary, the absolute values of $Z^*(O_{\perp})$ and $Z^*(\text{Sr})$ (figure 6(b)) decrease with increasing volume, indicating a decrease of long-range dipolar interaction of the Sr–O pair. As a result, the instability of the R_{25} mode in cubic SrTiO₃ is weakened at

expanded volume. For cubic BaTiO₃, the optimized lattice constant is 3.992 Å, which is much larger (about 2%) than that of SrTiO₃ (3.922 Å). Therefore, no AFD instability can be found, which has been confirmed by Ghosez [26]. However, the situation in SrTiO₃ is very different. When the volume is suppressed, the increasing repulsion between Ti and O atoms does not result in a significant increase of total energy of the system, as can be noted from figure 2 where the total energy decreases as the lattice constant decreases from 3.990 to 3.920 Å. The different volume dependence of total energy in the two compounds suggests that the smaller lattice constant of SrTiO₃ relative to BaTiO₃ is due to the Sr–O interaction. Moreover, because the valence configurations of Sr and Ba (4s²4p⁶5s² for Sr and 5s²5p⁶6s² for Ba) are very similar, the exclusive difference in ionic radius thus seems to be responsible for the different A–O interaction and lattice constants of the two compounds. To confirm the effect of ionic radius on the lattice constant, further investigations concerning the long-range and short-range interactions of the A–O (A = Sr, Ba) pair [26] are necessary. However, our results presented here indicate at least that the Sr–O interaction is crucial for the smaller lattice constant of SrTiO₃, which distinguishes the transition of SrTiO₃ from BaTiO₃.

4. Conclusion

Relying on the first-principles calculations, we have investigated the vibrational properties and potential energy curves of cubic SrTiO₃. At equilibrium volume (60.33 Å³), no FE instability is found, being consistent with further total energy calculations. However, an unstable R₂₅ mode corresponding to the AFD transition is observed. By investigating the phonons at different volumes, we found that the competition between the FE and AFD instabilities really exists. Our results also confirmed that increasing the crystal volume tends to suppress the AFD instability while enhancing the FE one. Finally, as the lattice constant of cubic SrTiO₃ is much smaller than for other ATiO₃ (A = Ba, Pb) compounds and further considering the volume dependence of the phonon frequency, we believe that the absence of the FE phase and the appearance of the AFD instability of cubic SrTiO₃ is due to its relatively small lattice constant.

Acknowledgments

The present work was supported by the National Natural Science Foundation of China (nos 20671032 and 20431030).

References

- [1] Fleury P A, Scott J F and Worlock J M 1968 *Phys. Rev. Lett.* **21** 16
- [2] Viana R, Lunkenheimer P, Hemberger J, Böhmer R and Loidl A 1994 *Phys. Rev. B* **50** 601
- [3] Sakudo T and Unoki H 1971 *Phys. Rev. Lett.* **26** 851
- [4] Müller K A and Burkard H 1979 *Phys. Rev. B* **19** 3593
- [5] Lasota C, Wang C Z, Yu R and Krakauer H 1997 *Ferroelectrics* **194** 109
- [6] Zhong W, King-Smith R D and Vanderbilt D 1994 *Phys. Rev. Lett.* **72** 3618
- [7] Martoňák R and Tosatti E 1994 *Phys. Rev. B* **49** 12596
- [8] Zhong W and Vanderbilt D 1996 *Phys. Rev. B* **53** 5047
- [9] Cohen R E 1992 *Nature* **358** 136
- [10] Piskunov S, Heifets E, Eglitis R I and Borstel G 2004 *Comput. Mater. Sci.* **29** 165
- [11] Chen Z X, Chen Y and Jiang Y S 2002 *J. Phys. Chem. B* **106** 9986
- [12] Hohenberg P and Kohn W 1964 *Phys. Rev.* **136** B864
- [13] Segall M D, Lindan P J D, Probert M J, Pickard C J, Hasnip P J, Clark S J and Payne M C 2002 *J. Phys.: Condens. Matter* **14** 2717

- [14] Perdew J P and Wang Y 1992 *Phys. Rev. B* **45** 13244
- [15] Monkhorst H J and Pack J D 1976 *Phys. Rev. B* **13** 5188
- [16] Baroni S, de Gironcoli S, Dal Corso A and Giannozzi P 2001 *Rev. Mod. Phys.* **73** 515
- [17] Ghosez Ph, Michenaud J P and Gonze X 1998 *Phys. Rev. B* **58** 6224
- [18] Weyrich K H and Siems R 1985 *Z. Phys. B* **61** 63
- [19] Fischer G J, Wang Z and Karato S I 1993 *Phys. Chem. Minerals* **20** 97
- [20] Dore P, Paolone A and Trippetti R 1996 *J. Appl. Phys.* **80** 5270
- [21] Gonze X, Ghosez Ph and Godby R W 1995 *Phys. Rev. Lett.* **74** 4035
- [22] Ghosez Ph, Gonze X and Michenaud J P 1998 *Ferroelectrics* **206** 205
- [23] Rabe K M and Waghmare U V 1995 *Phys. Rev. B* **52** 13236
- [24] Sai N and Vanderbilt D 2000 *Phys. Rev. B* **62** 13942
- [25] Zhong W and Vanderbilt D 1995 *Phys. Rev. Lett.* **74** 2587
- [26] Ghosez Ph, Cockayne E, Waghmare U V and Rabe K M 1999 *Phys. Rev. B* **60** 836